

Min Y. Yap,^a‡ Matthew C. J. Wilce,^a‡ Daniel J. Clayton,^b Patrick Perlmutter,^b Marie-Isabel Aguilar^a and Jacqueline A. Wilce^{a*}

^aDepartment of Biochemistry and Molecular Biology, Monash University, VIC 3800, Australia, and ^bSchool of Chemistry, Monash University, VIC 3800, Australia

‡ These authors should be considered joint first authors.

Correspondence e-mail:
jackie.wilce@monash.edu

Received 21 September 2010
Accepted 15 October 2010



© 2010 International Union of Crystallography
All rights reserved

Preparation and crystallization of the Grb7 SH2 domain in complex with the G7-18NATE nonphosphorylated cyclic inhibitor peptide

Grb7 is an adapter protein that is involved in signalling pathways that mediate eukaryotic cell proliferation and migration. Its overexpression in several cancer types has implicated it in cancer progression and led to the development of the G7-18NATE cyclic peptide inhibitor. Here, the preparation of crystals of G7-18NATE in complex with its Grb7 SH2 domain target is reported. Crystals of the complex were grown by the hanging-drop vapour-diffusion method using PEG 3350 as the precipitant at room temperature. X-ray diffraction data were collected from crystals to 2.4 Å resolution using synchrotron X-ray radiation at 100 K. The diffraction was consistent with space group $P2_1$, with unit-cell parameters $a = 52.7$, $b = 79.1$, $c = 54.7$ Å, $\alpha = \gamma = 90.0$, $\beta = 104.4^\circ$. The structure of the G7-18NATE peptide in complex with its target will facilitate the rational development of Grb7-targeted cancer therapeutics.

1. Introduction

The human growth factor receptor-bound protein 7 (Grb7) is a member of a family of adaptor proteins that include Grb10 and Grb14, which act to couple activated tyrosine kinases to downstream signalling pathways (Han *et al.*, 2001). Grb7-family proteins share a conserved multi-domain structure comprising of an N-terminal proline-rich domain, a Ras-associating-like (RA) domain, a pleckstrin homology (PH) domain, a region between the PH and SH2 termed the BPS domain and a C-terminal Src homology 2 (SH2) domain (Han *et al.*, 2001; Shen & Guan, 2004).

Upstream binding partners of Grb7 include focal adhesion kinases (FAKs) and members of the ErbB receptor family. Grb7 is present in focal adhesions, where it is bound and phosphorylated by FAK during cell migration (Han & Guan, 1999, 2000). In the cytoplasm, Grb7 usually binds to the cytoplasmic domain of the ErbB-3 receptor; however, studies have shown that in cancer cells Grb7 is associated with the ErbB-2 receptor, which plays a major role in cancer cell proliferation (Stein *et al.*, 1994). Grb7 is overexpressed together with ErbB-2 in breast cancer cell lines (Stein *et al.*, 1994), as well as in oesophageal and gastric carcinomas (Kishi *et al.*, 1997; Tanaka *et al.*, 1997).

The C-terminal SH2 domain of Grb7 mediates its binding to its interacting partners and forms the key recognition event necessary for triggering the unwanted downstream effects when Grb7 is overexpressed. SH2 domains are small modular domains which are able to bind to phosphorylated tyrosines in a sequence-dependent manner *via* a positively charged pocket on their surface (Bradshaw & Waksman, 2002; Waksman *et al.*, 1992) and recognize 3–6 residues immediately C-terminal to the phosphotyrosine (referred to as Y + 1, Y + 2 etc.) (Songyang *et al.*, 1993). The Grb7 SH2 domain has a strong preference for phosphotyrosines contained within a pYXN motif (Pero *et al.*, 2002) and forms a specific binding site for phosphotyrosines in the ErbB-2 receptor and FAK. The Grb7 SH2 domain is thus a prime target for inhibition, as blocking its activity would abolish the downstream effects of Grb7 when aberrantly overexpressed.

Using phage display, a nonphosphorylated peptide termed Grb7-peptide18-no arms thioether (G7-18NATE) was developed and found to be able to specifically bind to Grb7 SH2 and not to the closely related Grb14 or Grb2 SH2 domains (Pero *et al.*, 2002). Cell-permeable G7-18NATE has been shown to be able to selectively block the interaction of Grb7 and FAK *in vivo*, as well as to significantly reduce pancreatic cell migration and the proliferation of different breast cancer cell lines (Pero *et al.*, 2007; Tanaka *et al.*, 2006). As phosphotyrosines are unstable and reduce cell-wall permeability, the unphosphorylated G7-18NATE represents an attractive starting point for targeting Grb7 in the treatment of cancer. NMR studies have found that the G7-18NATE peptide has a tendency to form a turn around the YXN motif, but is otherwise a highly flexible molecule (Porter & Wilce, 2007).

To date, the structure of the Grb7 SH2 domain has been solved using crystallography to 2.1 Å resolution (PDB entry 2qms; Porter *et al.*, 2007). This structure shows that the Grb7 SH2 peptide binding site differs from other SH2 binding sites, with Ile522 blocking the Y + 3 position, and explains the preferential binding of Grb7 SH2 to G7-18NATE, which contains YXN in a turn confirmation (Porter *et al.*, 2007). Isothermal calorimetric experiments have been used to determine that G7-18NATE binds to Grb7 SH2 with micromolar affinity (Porter *et al.*, 2007). It is remarkable that a peptide inhibitor of this affinity displays cellular activity and suggests that a peptide with improved affinity may possess an even more potent bioactivity.

In order to develop G7-18NATE-based peptides that possess higher affinities for their target, we have undertaken crystallization of the G7-18NATE–Grb7 SH2 complex. This is anticipated to reveal the critical residues involved in the interaction and the structural basis for this interaction. We thus report the preparation of the G7-18NATE peptide in complex with the Grb7 SH2 domain and the formation of diffracting crystals for structure determination using X-ray crystallography.

2. Methods and results

2.1. Overexpression and purification of the Grb7 SH2 domain

The pGex2T plasmid containing the Grb7 SH2 insert (residues 415–532 of human Grb7) was obtained from Dr Roger Daly (Janes *et al.*, 1997). Grb7 SH2 was expressed as a GST-fusion protein in *Escherichia coli* strain BL21 (DE3) *plysS* as described previously (Porter *et al.*, 2007). The overexpressed protein was isolated from the cellular supernatant after incubation with glutathione beads (GE Healthcare) overnight at 277 K. After washing the beads with wash buffer (PBS pH 7.4, 0.5% Triton X-100 and 1 mM DTT), the fusion protein was eluted off the beads with wash buffer containing 10 mM glutathione. Grb7 SH2 was cleaved from the GST with a final concentration of 5 U ml⁻¹ thrombin (Sigma) overnight at 277 K. The protein solution was dialysed against cation-exchange buffer [20 mM *N*-(2-hydroxyethyl)piperazine-*N*-ethanesulfonic acid (HEPES) pH 7.6, 20% glycerol and 1 mM DTT] and applied onto a HiTrap SP Sepharose XL cation-exchange column (GE Healthcare) equilibrated in the same buffer. The Grb7 SH2 domain was eluted using a linear gradient of 0–0.5 M sodium chloride in cation-exchange buffer over a volume of 20 ml. The semi-purified Grb7 SH2 domain was then dialysed into 50 mM 2-morpholinoethanesulfonic acid (MES) pH 6.6, 100 mM NaCl and 1 mM DTT and further contaminants in the protein solution were removed using a HiLoad 16/60 Superdex 75 column (GE Healthcare). The protein was then tested for purity using a 15% SDS-PAGE gel and concentrated to 10 mg ml⁻¹ as

determined spectrophotometrically from the A_{280} using an extinction coefficient of 8480 M⁻¹.

2.2. G7-18NATE synthesis

The G7-18NATE peptide (amino-acid sequence WFEGYDNT-FPC) was synthesized using standard solid-phase Fmoc chemistry (Chan & White, 2000) using a Liberty Microwave Peptide Synthesizer (CHEM corporation, Kamp-Lintfort, Germany) on a 0.1 mmol scale of synthesis using Rink Amide Resin (Sewald & Jakubke, 2002). The first residue was coupled manually. The required amount of Cys(tBu) was dissolved in a threefold excess of 0.5 M HBTU in synthetic grade DMF. Diisopropyl ethylamine (DIPEA) was added to catalyse the formation of the activated amino-acid ester. The preactivated Cys ester mixture was then coupled to the dry swollen resin. The cysteine-coupled resin was then transferred to a microwave peptide synthesizer, upon which the full G7-18NATE sequence was assembled. Difficult-to-couple amino acids such as Trp, Asn and Thr were double coupled. The activator base was 2 M DIPEA in *N*-methylpyrrolidone. Deprotection after each coupling was effected with 20% (v/v) piperidine in DMF/0.1 M HoBT (hydroxybenzotriazole). After the final Fmoc deprotection, the N-terminal amino group on the tryptophan was capped using a solution comprised of 171 mg chloroacetic acid anhydride dissolved in 2 ml synthesis-grade DMF and 160 µl DIPEA for 30 min at room temperature. After cleavage from the resin in TFA and workup of the crude peptide, the potential CO₂ adduct on the tryptophan residue was removed using an adduct-removal reagent composed of 10% acetic acid, 50% ACN/H₂O and purified using preparative RP-HPLC. The cyclization reaction was carried out in 100 mM NH₄HCO₃ adjusted to pH 8.00 and diluted with an equal volume of 100% acetonitrile for 1 h at room temperature. Mass-spectrometric analysis of the folded peptide confirmed the formation of the thioether bond with the characteristic chloride-ion loss. The folded peptide was repurified using preparative RP-HPLC and its structure and purity were confirmed by mass spectrometry and analytical RP-HPLC.

2.3. Complex formation and crystallization

G7-18NATE was added to Grb7 SH2 at a 2:1 molar ratio under conditions previously shown by NMR spectroscopy to result in complete complex formation in solution (Porter *et al.*, 2007). Crystallization screens were set up using a Honeybee crystallization robot (Genomic Solutions) and 96-well Intelli-Plates (Art Robbins Industries) with drops consisting of 100 nl sample solution added to 100 nl reservoir solution. The initial screens for crystallization conditions were performed using commercially available kits from Sigma-Aldrich, Hampton Research and Jena Bioscience. Crystals formed within 2 d in condition Nos. 47, 82, 83, 84 and 98 of Index screen (Hampton Research) at room temperature. These conditions were optimized using the hanging-drop vapour-diffusion method, in which 1 µl protein/peptide solution was added to 1 µl reservoir buffer, and crystals appeared in screens set up around condition Nos. 82, 83 and 84, all of which contained magnesium chloride in the reservoir buffer. The crystals formed appeared to be small thin plates that were stacked on each other. In order to try to slow the growth of the crystals, 10% (w/v) glycerol was added to the reservoir buffer. Further optimization was performed using Additive Screen (Hampton Research), in which 0.2 µl additive solution was added to 0.9 µl protein/peptide solution and 0.9 µl reservoir buffer. The final optimized condition consisted of 17.5% (w/v) PEG 3350, 0.2 M MgCl₂, 0.1 M glycine, 10% (w/v) glycerol and 0.1 M bis-tris pH 6.0.

Table 1

Crystallographic data-collection statistics for the Grb7 SH2–G7-18NATE complex.

Values in parentheses are for the highest resolution shell.

Space group	$P2_1$
Unit-cell parameters (Å, °)	$a = 52.7, b = 79.1, c = 54.7, \alpha = 90.0, \beta = 104.4, \gamma = 90.0$
Resolution (Å)	37.42–2.41 (2.48–2.41)
No. of reflections	30241 (10904)
No. of unique reflections	15617 (1027)
Multiplicity	1.9 (1.9)
Completeness (%)	93.1 (84.3)
$\langle I/\sigma(I) \rangle$	7 (2)
$R_{\text{merge}}^{\dagger} (\%)$	9.6 (43)
$R_{\text{p.i.m.}}^{\ddagger} (\%)$	9.4 (42)

$\dagger R_{\text{merge}} = \sum_{hkl} \sum_i |I_i(hkl) - \langle I(hkl) \rangle| / \sum_{hkl} \sum_i I_i(hkl)$, where $I_i(hkl)$ is the intensity of individual reflections. $\ddagger R_{\text{p.i.m.}}$ is the multiplicity-weighted R_{merge} .

2.4. Data collection

Diffraction data were collected at the Australian Synchrotron (to 2.4 Å resolution). A single crystal was picked up using a Hampton cryoloop, streaked through a solution containing 25% glycerol in the reservoir solution and flash-cooled at 100 K. X-ray diffraction data were collected on the high-throughput protein crystallography beamline at the Australian Synchrotron using an ADSC Quantum 210 detector. 91 diffraction images were recorded. The oscillation angle for each frame was 1° and the exposure time was 1 s. The diffraction data were integrated using *MOSFLM* (Leslie, 1999) and the intensities were merged and scaled using *SCALA* (Collaborative Computational Project, Number 4, 1994). Wilson scaling was applied using *TRUNCATE* (Collaborative Computational Project, Number 4, 1994).

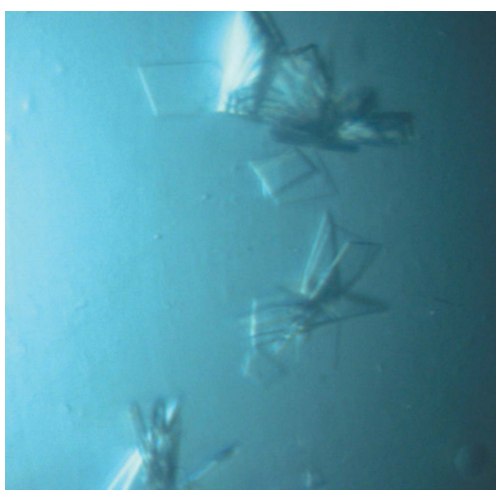
3. Results and discussion

The G7-18NATE peptide was synthesized and combined in a ratio of 2:1 (*i.e.* excess peptide) with the purified Grb7 SH2 domain at 10 mg ml⁻¹. This ratio was chosen in order to shift the equilibrium towards the formation of 100% Grb7 SH2 domain in complex with the peptide, at the risk of the excess peptide inhibiting crystal formation. In addition, since the Grb7 SH2 domain–G7-18NATE complex was highly soluble, it was important to undergo crystallization trials at this high concentration. Dilution of the protein was

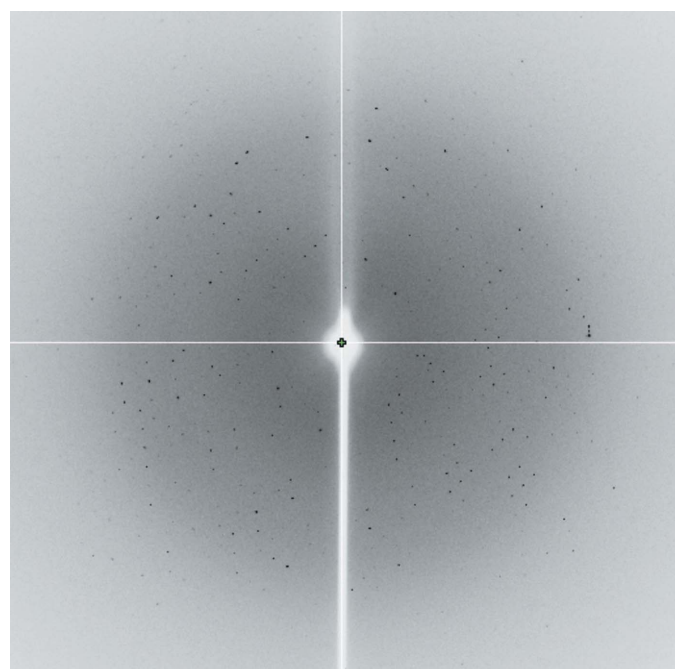
avoided by adding protein solution directly to the lyophilized and pre-weighed peptide. No further purification of the complex was undertaken as it was considered desirable to maintain excess peptide. Crystallization conditions were obtained from standard screens and were further optimized through the use of glycerol to slow down the rate of crystal growth and through screening additives. The finding that the optimum condition for crystallization was at pH 6.0 is consistent with the pH-sensitivity of the interaction of the Grb7 SH2 domain with G7-18NATE. In a recent study, we determined a 100-fold higher affinity of this interaction at pH 6.0 compared with pH 7.4 (Gunzburg *et al.*, 2010).

The crystals grown under the optimized condition were plate-like with dimensions of 0.01 × 0.06 × 0.1 mm (Fig. 1) and could be used for the collection of high-quality diffraction data (Fig. 2) on the Australian Synchrotron protein beamline (MX1). Diffraction data are summarized in Table 1. The diffraction data were consistent with space group $P2_1$. Starting phases have been found by molecular-replacement techniques using *Phaser* (McCoy *et al.*, 2007) and the coordinate set previously determined in our laboratory for the Grb7 SH2 apo protein (PDB code 2qms). The electron density clearly revealed the presence of the G7-18NATE peptide bound to each Grb7 SH2 domain dimer and of four Grb7 SH2 domain molecules in the asymmetric unit. Based upon the known molecular weight of the Grb7 SH2–G7-18NATE complex of 15 089 Da, the presence of four molecules in the asymmetric unit corresponds to a Matthews coefficient of 1.83 Å³ Da⁻¹ and a solvent content of 32.76%.

The structure of the complex of the Grb7 SH2 domain with the G7-18NATE inhibitor will provide valuable information as to the basis of its affinity and specificity. In particular, it will be of interest to compare the interaction of the G7-18NATE peptide with the Grb7 SH2 domain with the previously reported interaction of a phosphorylated peptide, representing a natural target peptide, with the Grb7 SH2 domain solved using NMR spectroscopy (Ivancic *et al.*, 2003). The G7-18NATE inhibitor has already demonstrated biological activity in cancer cells despite its relatively low affinity for its

**Figure 1**

Crystals of the Grb7 SH2–G7-18NATE complex of approximately 0.01 × 0.06 × 0.1 mm in size.

**Figure 2**

A representative diffraction image acquired from a Grb7 SH2–G7-18NATE complex crystal.

target (Pero *et al.*, 2007; Tanaka *et al.*, 2006). The structure of the complex will play a key role in the discovery of second-generation inhibitors of potentially high affinity for the Grb7 target and that are more potently antitumorigenic.

We wish to thank the staff at the Protein Crystallography Beamline (MX1) at the Australian Synchrotron, Victoria, Australia where the diffraction data were collected. This work was supported by the Department of Biochemistry and Molecular Biology at Monash University, a grant from the Australian Research Council awarded to JAW and a National Health and Medical Research Senior Research Fellowship awarded to MCJW.

References

Bradshaw, J. & Waksman, G. (2002). *Adv. Protein Chem.* **61**, 161–210.

Chan, W. C. & White, P. D. (2000). *Fmoc Solid Phase Peptide Synthesis: A Practical Approach*. Oxford University Press.

Collaborative Computational Project, Number 4 (1994). *Acta Cryst. D* **50**, 760–763.

Gunzburg, M. J., Ambaye, N. D., Hertzog, J. T., Del Borgo, M. P., Pero, S. C., Krag, D. N., Wilce, M. C. J., Aguilar, M.-I., Perlmutter, P. & Wilce, J. A. (2010). *Int. J. Pept. Res. Ther.* **16**, 177–184.

Han, D. & Guan, J. (1999). *J. Biol. Chem.* **274**, 24425–24430.

Han, D. & Guan, J. (2000). *J. Biol. Chem.* **275**, 28911–28917.

Han, D., Shen, T. & Guan, J. (2001). *Oncogene*, **20**, 6315–6321.

Ivancic, M., Daly, R. J. & Lyons, B. A. (2003). *J. Biomol. NMR*, **27**, 205–219.

Janes, P., Lackmann, M., Church, W., Sanderson, G., Sutherland, R. & Daly, R. (1997). *J. Biol. Chem.* **272**, 8490–8497.

Kishi, T., Sasaki, H., Akiyama, N., Ishizuka, T., Sakamoto, H., Aizawa, S., Sugimura, T. & Terada, M. (1997). *Biochem. Biophys. Res. Commun.* **232**, 5–9.

Leslie, A. G. W. (1999). *Acta Cryst. D* **55**, 1696–1702.

McCoy, A. J., Grosse-Kunstleve, R. W., Adams, P. D., Winn, M. D., Storoni, L. C. & Read, R. J. (2007). *J. Appl. Cryst.* **40**, 658–674.

Pero, S., Oligon, L., Daly, R., Soden, A., Liu, C., Roller, P., Li, P. & Krag, D. (2002). *J. Biol. Chem.* **277**, 11918–11926.

Pero, S., Shukla, G., Cookson, M., Flemer, S. J. & Krag, D. (2007). *Br. J. Cancer*, **96**, 1520–1525.

Porter, C., Matthews, J., Mackay, J., Pursglove, S., Schmidberger, J., Leedman, P., Pero, S., Krag, D., Wilce, M. & Wilce, J. (2007). *BMC Struct. Biol.* **7**, 58.

Porter, C. & Wilce, J. (2007). *Biopolymers*, **88**, 174–181.

Sewald, N. & Jakubke, H.-D. (2002). *Peptides: Chemistry and Biology*, p. 212. Weinheim: Wiley-VCH.

Shen, T. & Guan, J. (2004). *Front. Biosci.* **9**, 192–200.

Songyang, Z. *et al.* (1993). *Cell*, **72**, 767–778.

Stein, D., Wu, J., Fuqua, S., Roonprapunt, C., Yajik, V., D'Eustachio, P., Moskow, J., Buchberg, A., Osborne, C. & Margolis, B. (1994). *EMBO J.* **13**, 1331–1340.

Tanaka, S., Mori, M., Akiyoshi, T., Tanaka, Y., Mafune, K., Wands, J. & Sugimachi, K. (1997). *Cancer Res.* **57**, 28–31.

Tanaka, S., Pero, S., Taguchi, K., Shimada, M., Mori, M., Krag, D. & Ariis, S. (2006). *J. Natl Cancer Inst.* **98**, 491–498.

Waksman, G., Kominos, D., Robertson, S. C., Pant, N., Baltimore, D., Birge, R. B., Cowburn, D., Hanafusa, H., Mayer, B. J., Overduin, M., Resh, M. D., Rios, C. B., Silverman, L. & Kurian, J. (1992). *Nature (London)*, **358**, 646–653.